International Journal Of
Industrial Electronics Control and Optimization
Print ISSN: 3517-2645
Online ISSN: 3568-2645
Homepage: https://ieco.usb.ac.ir/

Thermal Comfort-Based Heat Pumps Utilization for Wind Power Uncertainty Management

Mohammadmehdi Sedaghatzadeh[1] | Mohsen Gitizadeh[2] Saeed Hasanvand[3]

Department of Electrical and Electronics Engineering, Shiraz University of Technology, Shiraz, Iran[1,2].
Department of Electrical Engineering, Firouzabad Institute of Higher Education, Firouzabad, Fars, Iran[3].
Corresponding author's email: Gitizadeh@sutech.ac.ir

Article Info

Article type:
Research Article

Article history:
Received: 2023- February-24
Received in revised form: 2023- June-09
Accepted: 2023- June-1
Published online: 2023- June-1

Keywords:
Congestion,
Distribution system,
IGDT
Renewable energy,
Uncertainty management,

ABSTRACT

Objective: Demand response programs (DRPs) are considered a promising solution to address the variability and uncertainty of renewable generations. Heat pumps (HPs) as responsive loads are prone to participate in DRPs. HPs participation in DRPs will lead to changes in the buildings' temperature and, correspondingly, the occupants' thermal comfort (OTC). If these programs are not planned wisely, HPs owners' tendency to participate in DRPs will reduce, and power system operators will be deprived of the DRPs benefits. This work proposes a new ASHRAE55-based framework to guarantee the OTC. Information gap decision theory (IGDT) is also used to address the uncertainty of renewable generation. Then, an objective function is defined to simultaneously optimize the power consumption of HPs and the uncertainty of wind turbine generators. To find the optimal solution, the standard and adaptive fuzzy PSO algorithms are used. For determining the participation of HPs in the DRPs, there is a conventional scenario in which the temperature of each residence should be limited to the range defined by the occupant(s). The simulation results verify the superiority of the proposed scenario over the conventional one.

Nomenclature

DG	Distributed generation
DSO	Distribution system operator
$DRPs$	Demand response programs
DLC	Direct load control
HPs	Heat pumps
$IGDT$	Information gap decision theory
MIT	Massachusetts Institute of Technology
OTC	Occupants' thermal comfort
PMV	Predicted mean Vote
PSO	Particle swarm optimization process
RA	Risk-averse strategy
RS	Risk-seeker strategy
$TABS$	Thermally Activated Building System
VFD	Variable frequency drive
$VSHPs$	Variable speed heat pumps
$TABS$	Thermally Activated Building System
VFD	Variable frequency drive
$VSHPs$	Variable speed heat pumps
WT	Wind turbin
A	Area of room surface (m^2)
COP	Compressor coefficient of performance
csh_c	Specific heat capacity [J/kg.K]
h	Convective heat transfer coefficient [W/(m2.K)]
Icl	Clothing insulation[m2°C/W]
k	Clothing insulation[m2°C/W]
k_ω, k_C, k_e	VSHP steady state linear model coefficients
L	Thickness of the room surface (m)
k_{offset}	VSHP steady state linear model coefficients

Copyright © Sedaghatzadehat al.
Publisher: University of Sistan and Baluchestan

R_{cv}	Convective resistance[m2 K w-1]	X	Vector of decision variables
R_{cd}	Conductive resistance[m2 K w-1]	$\bar{\psi}$	Predicted value of the uncertain parameter
T_{e-air}	Ambient temperature [°C]	ψ	Realized value of the uncertain parameter
T_{C-amb}	Outdoor air temperature [°C]	α	Uncertain radius of uncertainty
ρ	Density of the surface materials [kg/m3]]	$\hat{\alpha}$	Maximum radius of uncertainty
ω_r	Compressor speed [rad/s]	H	Vector of inequality constraints
$P_{HPs,n}$	Heat pumps consumption in bus no.n [kW]	Γ	Set of all equality and inequality constraints
P_{min}	Heat pump minimum consumption [kW]]	G	Vector of equality constraints
P_{max}	Heat pump maximum consumption [kW]	Λ	Critical value of the objective function
P_{max}	Heat pump maximum consumption [kW]	P_{net}	Network power provision [kW]
$P_{T_{min}}$	Heat pump consumption correlated to T_{min}[kW]	P_{loss}	Network power loss[kW]
$P_{T_{ideal}}$	Heat pump consumption correlated to T_{idea}l[kW]	P_{HPs}	HPs power consumption[kW]
T_{min}	Indoor air temperature correlated to PMV=-0.5 [℃]	$\overline{W_T}$	Predicted value of the WT active power generation
T_{ideal}	Indoor air temperature correlated to PMV=0 [℃]	CI	Congestion index [MVA]
T_{max}	Indoor air temperature correlated to PMV=+0.5 [℃]	CI_C	Critical value of the CI [MVA]
f	Objective function	S_L	Power flow in line L [MVA]
		S_{Lmax}	Maximum power flow in line L [MVA]
		M	Metabolic Rate[met]
		P_m	Compressor mechanical input power [kW]
		Q_{hp}	Heat pump thermal energy [kW]

I. Introduction

The global warming phenomenon and its devastating effects have compelled many countries to sign international agreements to clear the way for the world's energy policy. The Paris Agreement [1] is a landmark in this regard. Decarbonizing the power sector by increasing the integration of renewable energy and electrification of transportation and heating/cooling sectors should be considered as two steps to implement the agreements. Solar photovoltaic and wind turbines have experienced the fastest expansion among different renewable generation technologies. These technologies accounted for 90% of the new renewable generating capacity in 2022. However, the rising penetration level of renewable energy sources leads to the mismatch between renewable supply and demand because of the unpredictable and variable nature of wind and solar resources. One option to address the problem is to shift the paradigm of energy use and production from "production p Within the UK domestic sector, space and water heating comprise 80% of the energy consumption. Furthermore, by 2030, the UK might have 9 million Heat Pumps (HPs), shifting a portion of heating energy resources from gas to electricity. A survey found that nearly 90 percent of American households have HPs of some sort; hence, these loads have a high potential to be deployed by demand response programs (DRPs).ursuing demand" to "demand pursuing generation". Therefore, one promising DRPs option is HPs consumption control for managing the uncertainty and curtailment of renewable energy resources [2, 3]. This paper investigates the effect of using HPs in managing wind power uncertainty. Controlling the consumption of HPs in the form of DRPs affects the temperature of people's living/working environment and their thermal comfort.

Therefore, the thermodynamic model of residences should also be considered. Since a few numbers of papers simultaneously examined three topics including the OTC, uncertainty management, and buildings thermal networks, the review of references has three subsections including uncertainty management, OTC, and thermodynamic models of buildings.

a) OTC related publications: From the OTC perspective, three different visions were investigated by authors:

• Feedback based: In this category, the data from an experimental room provided the main foundation of the method. With the aid of a supervisory control strategy called smart zoning in every room of the building, set points were regulated so that the whole building's performance was optimized from energy consumption and OTC perspectives [4]. In [5], a two-level supervisory closed-loop feedback strategy was exploited. At the first level, each building used a local closed-loop feedback controller that only analyzed local measurements; at the upper level, a centralized unit monitored

updated the local controllers to optimize energy cost and thermal comfort. Anand et al. [6] utilized three occupancy-based HPs operational strategies to optimize energy consumption and indoor air quality when a typical variable air volume system served multiple zones inside a building. Based on the duration residents occupied a specific room, the amount of air entering the area and the temperature were set. In the abovementioned references, OTC was utilized only to prove the effectiveness of the proposed methods and not as their foundation. Moreover, the main reason for HPs introduction into electrical surveys is their remedial capability in the future operational issues of renewable-dominated energy systems. Therefore, ignoring operational objectives, constraints, and interactions of these loads with power systems (especially low-voltage grids) would not be appropriate. Moreover, as each occupant would have his behavior or each room in a building could have a different occupancy pattern, the control algorithm will be too elaborate for distribution system operator (DSO) or load aggregator to adopt for a large number of HPs.

• Consumer ideal temperature range: For the day-ahead and intra-day scheduling of the operation of heating units within a city section, Diekerh et al. [7] used a hierarchical robust distributed optimization algorithm. The paper concentrated on optimization methods, and each consumer introduced a separate objective function (OF) to be optimized. In [8], considering self-defined occupant thermal comfort, a mixed-integer linear programming approach provided optimal scheduling for electrical loads in a smart building. The OTC defined the degree of flexibility offered by the HPs. A consumer could define the degree of flexibility; however, it should be determined by the DSO so that OTC is assured while operational and power market issues are managed. Marco Pau [9] quantified customer flexibility with an optimization method. Each consumer introduced an ideal range for temperature variations.

• OTC ignorance: An economic model of predictive control was proposed in [10] to explore how district heating companies can use power-to-heat devices and traditional central cogeneration to balance the generation and consumption of electric energy in smart grids. The authors of [11] proposed a method that controls HPs based on local price to avoid the overload in systems; however, they ignored the OTC. Mendeza et al. [12] represented a control model for HPs. DR signals from the power market altered the loads' thermal setting to improve the magnitude of the network voltage; however, the effect of HPs set points alteration on the OTC was not investigated. The authors of [13] introduced an aggregated electro-thermal model for a group of houses. Energy consumption moved in time to balance the grid. Thermal discomfort was permitted. They considered large energy storage capacities to shift energy consumption to the periods in which high penetration of renewable energy sources happened. In [14], no calculation was carried out to understand if users-defined thermal comfort is following their real thermal needs. An optimization procedure achieved coincident power peak shaving in the distribution grid and provided the required thermal comfort for end-users. Kim et al. [15] modeled the thermal dynamics of variable speed heat pumps (VSHPs) using a set of piecewise linear equations for two different methods of room temperature control; however, the results were so contingent upon how an occupant defined his suitable thermal comfort. Abyaneh et al. [16] introduced a probabilistic nonlinear model for maximizing multi-energy storage and demand response flexibility. The proposed model has provided adjusted temperatures for consumers. The temperature was not based on occupants' real thermal needs, and no specific index was proposed for evaluating the OTC.

• b) Uncertainty related studies: In [17], to obtain the optimal locations of wind power plant installation, the uncertainty of electrical loads and wind power and their correlation have been considered. Considering the correlation between hourly loads and wind power variations mitigates the mismatch between the load profile and wind power. Malekijavan et al. have proposed a method to optimize the operating and reliability costs of an energy hub while considering uncertainties of loads, energy price, electrical vehicle demand, and equipment availability [18]. In this study, the OTC is ignored to be considered as a constraint in the optimization problem. In [19] micro-grid operation was optimized by considering reliability, flexibility, and environmental constraints. In this study, the renewable energy generation uncertainty was addressed using stochastic programming. The optimal energy management and operation of networked microgrids using dispatchable (fuel cell and microturbine) and non-dispatchable units (wind turbine and solar units) have been investigated by Vosoogh et al. [20]. In this study, a stochastic framework has been utilized to solve the optimal economic dispatch of the units and investigate the uncertainty effects of renewable energy resources, electric vehicles, and load demand. The abovementioned references utilize stochastic planning methods to deal with uncertainties of renewable generations which were not as helpful as the IGDT when micro-grids are subject to severe uncertainty. In [21] a multi-timescale economic scheduling model considering the uncertainty of wind power has been proposed. Day-ahead, intraday, and real-time scheduling periods were considered in which wind power prediction accuracy was improved, and optimal planning was carried out using the appropriate methods. In the presented model, the prediction error range must be specified in advance. Otherwise, the model will not be applicable, and the IGDT should be substituted for the proposed method. In [22], the interval optimization method considers the uncertainty of wind power and photovoltaic units in a combined cooling, heating, and power system. The advantage of this study is that, in addition to the energy cost, carbon oxide emissions are also minimized. The interval

optimization method requires the lower and upper limits of uncertainty parameters. So, this method is impossible to implement without knowing these boundaries. Authors in [23] minimize the total energy cost of the multi-carrier microgrids and decrease CO2 emission rates by considering HPs. Uncertainties associated with a wind turbine (WT), electrical loads, electricity market price, and behavior of the electric vehicle are considered. Coelho et al. propose an optimization model to use the flexibility of multi-energy systems to mitigate the uncertainty associated with wind generation [24]. Correa et al. present an optimization model for home energy management systems while the uncertainty of energy prices, PV production, and load are considered [25]. OTC has been ignored in all the above-mentioned references. Probability density or the membership function-based, IGDT-based and hybrid-based frameworks were proposed in researches to deal with the renewable energy resources uncertainty. In a network with severe uncertainty in the wind power profile, the IGDT-based method was proved to be more effective with less computational burden [26]. In [27], a hybrid stochastic/IGDT approach is utilized to optimally schedule a wind-based energy hub and manage the electricity price uncertainty while the OTC was ignored. Murphy et al. study both opportunistic and conservative effects of a WT uncertain generation on the standard distribution system congestion [28]. Fixed integrated pre-determined multi-level of load flexibility has been assigned to the nodes (one node for each level of flexibility) with the dominant effect on the congestion (as the OF) to exhibit the effectiveness of the DRPs on uncertainty management problem. A two-step optimal operating procedure for a community-integrated energy system was presented by Wang et al., addressing multiple uncertainties and integrated demand response [29]. In [30], a stochastic framework for residential energy management in multi-carrier buildings has been proposed. Thermal and electrical loads are categorized as price-responsive and non-responsive loads. The authors of [31] consider the electrical chiller as the cooling supplier of an office building. A two-step hierarchical microgrid energy management method for an office building is proposed that accounts for uncertainties from renewable generation, electric load demand, outdoor temperature, and solar irradiance while ignoring the OTC impacts on the system flexibility. A resilience-oriented stochastic framework considering integrated demand response is proposed in [32] to improve the overall economy and system resiliency, whereas HPs' high potential for managing uncertainty is ignored.

• c) Thermodynamic models for buildings: Simplified dynamic models of buildings are gaining more and more attention recently. TABULA and EPISCOPE are two European projects that provided a compatible structure for classifying building types and constructing building archetypes based on statistical analyses of large building samples [33]. Detailed analyses of buildings' models are proposed in [34-36] as well as international standard ISO 13790 and the German Guideline VDI 6007. The system domain in these models is approximated by a series of nodes connected by thermal resistances and capacitances. Their main advantage is that once the parameters are identified, the system can be solved analytically, avoiding the problems that arise in numerical schemes. In [34] an elaborated thermodynamic model of an experimental room is introduced. The reference did not study the distribution system operational limits and system-wide effects of HPs consumption alteration. The model is developed in [35] for HPs control methods investigations. In [36], reduced-order thermal response models of twelve representative German building types in three insulation states were proposed. The DRPs potential of the buildings' structural thermal mass (called passive storage) was used in two predefined cases. In the discharge case, HPs are actively switched off, while the heat demand is covered by the passive storage discharge. In charge case, HPs are actively switched on regardless of the current heat requirements by overheating the passive storage. HPs have an on-off controller which is an old control method and could create power quality consequences, especially if the degree of HPs penetration grows in the future; 20℃ to 22℃ is considered as the comfort band without introducing any criterion.

In the abovementioned references, RC models are used for the electro-thermal simulation of buildings. Consequently, each model can be selected to demonstrate the effectiveness of the proposed method in WT uncertainty management. The thermal network introduced in [34] is a thermodynamic model modified for electrical applications. Therefore, the model is utilized by this paper for the investigations of the building's thermal behavior.

ASHRAE55 standard [37-38] creates a framework for the OTC determination that depends on occupants' physical and environmental status. In other words, this standard will transform the OTC from a personal interpretation-based factor to a measurable and calculable one. This work evaluates temperature ranges that guarantee the OTC. Consequently, DSO would count on steady and maximum HPs flexibility to overcome operational problems and postpone low voltage grids' future expansion. HPs consumption is a decision variable in this work's optimization algorithm rather than the source of uncertainty. HPs consumption control is considered a tool to save/benefit the DSO and the low voltage network to a specific level of decrease/increase in the WT power generation. Finally, DSO with direct load control (DLC) signals changes HPs set points or consumption in each bus of the test system. The contributions of this study are summarized as follows:

• Based on the ASHRAE55 standard and RC-network representations of examined building models, a new OTC-ensured HPs DRPs participation framework is proposed to introduce the loads as tools of WT uncertainty management.

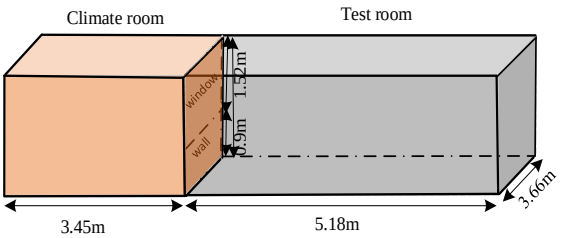


Fig1. Experimental room.

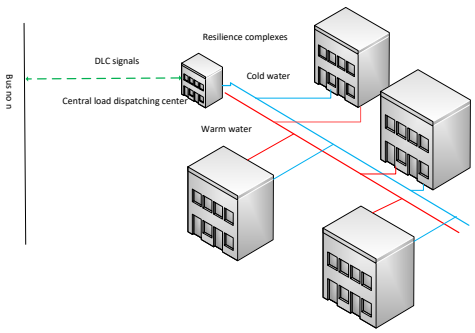


Fig2. Heat loads in a bus.

• The core of the IGDT method is an OF which is used for optimizing the permissible renewable energy forecast error.

This work adds a HPs consumption-related term to the function which has a positive influence on the forecast.

The rest of this paper is organized as follows. System modeling, thermal comfort and calculation of OTC-assured HPs consumption boundary are explained in section 2. The IGDT and optimization process are proposed in section 3. Simulation results are depicted in section 4. Finally, the conclusion is drawn in the last section.

II. System modeling

A. MIT experimental room' thermal network

The building is located at MIT and divided into two parts: Climate Room and Test Room. The outdoor temperature changes are simulated by changing the climate room temperature. The test room is equipped with Thermally Activated Building System (TABS) ventilation system (Fig.1). The system provides resilience complexes with warm water. Hot water pipes pass through the floor. The walls are made of layers of thermal insulation and concrete. Each layer is defined by its thickness, thermal conductivity, specific heat capacity, and density. The test room has a heater and lighting. The heat generated by these sources simulates thermal losses.

In this work, DLC signals, via a Variable Frequency Drive (VFD), control compressor speed, rate of the working fluid, and power consumption of a VSHP in a central load dispatching center or local control center (Fig.2). The signals are applied according to the DSO operational /power market goals, while the indoor air temperature is maintained at hourly based, OTC-assured limits. All residents' complexes are assumed to have the same structure as the experimental room.

In Fig.3 thermal network of the room is introduced. Conductive and convective resistances are modeled by electrical resistances. The electrical equivalent of temperature is the voltage source, and heat gains are modeled by voltage and current sources, respectively [35]. Qhp is the thermal energy injected into the building, and Te-air is the operative temperature. The values of convective thermal resistance (Rcv), conductive thermal resistance (Rcd), and thermal capacitance (C) could be obtained via (1)-(3).

$$Rcd = L.(k.A)^{-1} \quad (1)$$

$$Rcv = (h.A)^{-1} \quad (2)$$

$$C = c_{shc}.L.A.\rho \quad (3)$$

L and A are the thickness and area of the room surface, respectively. ρ and cshc are the density and specific heat capacity of the surface materials. Also, k and h are the conductive and convective heat transfer coefficients; indeed, h is set to 5W/ (m2.K), regardless of the surface characteristics, although all the convective resistors are denoted as Rcv. All parameters in the RC model are calculated based on the experimental room characteristics proposed in [34].

B. Occupants' thermal comfort

Thermal comfort is a mental state that expresses the degree of satisfaction of a person from the thermal conditions of the environment. There are several physical parameters involved in thermal comfort. Two conditions must be fulfilled to create thermal comfort: 1-The composition of the temperature produced inside the body and the skin temperature create a neutral thermal sensation (not cold or warm), and 2- The energy balance is created in the body, which means that the heat generated by the metabolism is equal to the temperature exchanged between the body and the environment. Relationships between skin temperature parameters, the degree of heat inside the body, and the amount of physical activity create a neutral sense of warmth in experimental studies. In these experiments, transpiration rate and skin temperature are measured for different amounts of body metabolism, while the person under the test has thermal comfort in all conditions. What makes looking into thermal comfort vital is its remarkable impact on residents' satisfaction with consistent DRPs participation. Therefore, HPs DRPs will be reduced if the OTC is ignored by the DSO.

Predicted Mean Vote (PMV) is a seven-point scale for heat sensation. This index allocates a number for the degree of thermal sensation of individuals. According to an occupant's clothing, metabolism, and physical conditions, the room temperature equals a specified PMV. PMV could be positive or negative. The positive values of the table (1) are equivalent to the temperatures in which the residents feel a little heat, and the negative values of the table correspond to the temperatures that will cause the residents to feel a little cold. The ideal residence's temperature is the one that occupants feel

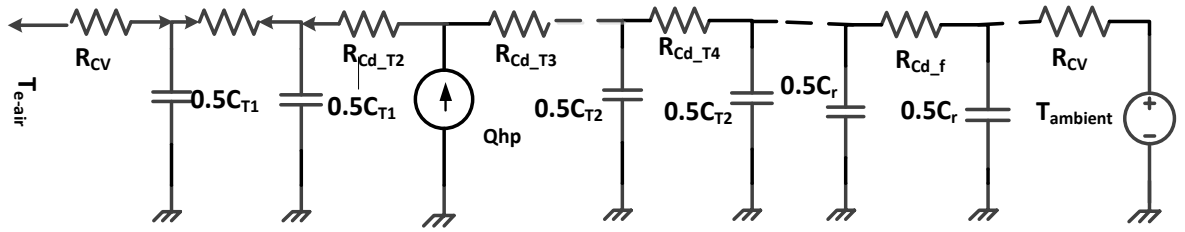


Fig.3. Electro-thermal network of the experimental room.

TABLE 1
PMV AND THERMAL SENSATION

PMV	THERMAL INDICATION
+3	Too warm
+2	Warm
+1	A little warm
0	Neutral
-1	A little cold
-2	Cold
+3	Too warm
+2	Warm
+1	A little warm
0	Neutral

thermally neutral. The ASHRAE55 standard introduces (4) as the allowable range for PMV deviation from the ideal value (PMV=0).

$$-0.5 \le PMV \le +0.5 \qquad (4)$$

In the following section, the temperature range in which the constant regulation of the indoor air temperature ensures the OTC is determined (the temperature range equivalent of (4)).

For the internal space temperature of a house, this work defines 'Tideal' as a temperature in which the PMV index is zero; 'Tmin' is the minimum permissible temperature in which PMV=-0.5 and occupants feel a tolerable sense of coldness, and 'Tmax' is the maximum allowable temperature in which PMV=+0.5 and occupants have an endurable sense of warmth. Tmin, Tmax, and Tideal are determined using a relationship between the operative temperature and PMV [37- 39].

C. OTC-assured temperature boundary

PMV equation is denoted as follows:

$$PMV = f\left(T_{e_air}, t_r, M, W, I_{cl}\right) \qquad (5)$$

Two different groups of information should be provided:

• Occupants' physical characteristics include their metabolic rate (M), effective mechanical power (W) that is dependent on the type of activity, and thermal insulation of occupants' clothing (Icl).

• Environmental characteristics include airspeed, relative humidity, operative temperature (Te_air), and mean radiant temperature (tr). Te_air describes the combined effects of convective and radiant heat transfer, and tr shows the radiation temperature of surrounding surfaces.

Most of the needed parameters could be estimated by statistical methods. In system-wide investigations, the number of HPs is high, and each occupant would feel thermal discomfort even if the indoor temperature is maintained in the OTC-assured boundary (Eq.5); therefore, in this work, a day is divided into three time periods. In each period, all effective parameters on residents' sense of warmth, except HPs injected thermal energy (Qhp), are assumed to have minimum possible values defined by the standard (Table.2). The assumptions are:

TABLE 2
TYPICAL CLOTHING INSULATION AND ACTIVITY

Time period	ICL	Residents' clothes	M	Resident's activity
10PM-7AM	1	Typical winter indoor clothing	40	Sleeping
8AM-4PM	0.85	Long sleeve shirt	65	Typing
5PM-9PM	0.96	Sleep wear pajama tops	100	Housework
5PM-9PM	0.96	Sleep wear pajama tops	100	Housework

• The mean radiant temperature is assumed to be the minimum ASHRAE55-defined value (10℃). In this way, the effect of residents surrounding objects in heating the building is minimized; especially in the daytime, the radiant temperature is higher than 10℃, and residents' sense of warmth increases. In other words, HPs are assumed as the only means of providing thermal energy for residents.

• Tables in Appendix B of the ASHRAE55 standard are used to estimate the clothing insulation parameter (Icl). The maximum value of the parameter is 1, which represents typical winter indoor clothing. For the period between 9 PM-7 AM, Icl is assumed to be 1. Usually, at night time residents wear clothes with higher insulation values. For example, using a multi-purpose quilt and wearing full-slip sleepwear at night can raise the Icl to 4.56 [40]; the PMV and thermal sensation of occupants will be more than what is considered by the DSO.

• The parameters related to the weather have been selected based on Tehran's monthly and annual statistics [41-42].

• For 9 PM-7 AM and 5 PM-9 PM periods, archetypal activity levels (M) are supposed for occupants. From 8 AM to 4 PM, an activity with a low metabolic rate is assumed for occupants. More common daytime activities increase the metabolic rate, PMV, and occupants' thermal sensation. Based on the above assumptions and Eq.4, Tmin, Tideal, and Tmax are calculated and depicted in Fig.4.

The operative temperature should be held at the boundary

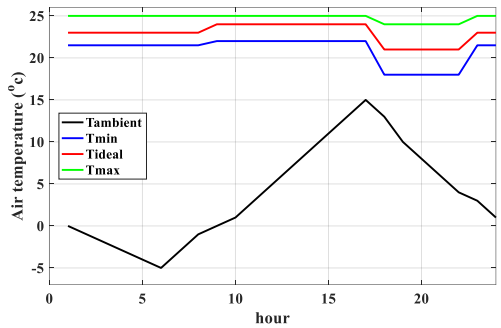


Fig4. Tmin, Tideal and Tmax in a winter day.

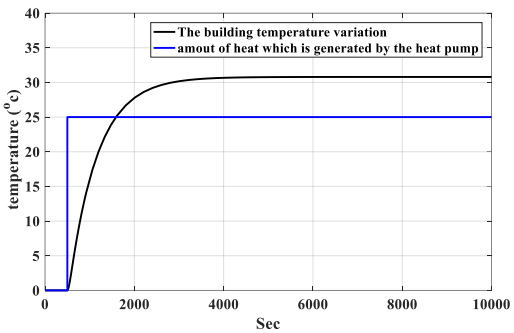


Fig. 5. *Step response of the building*.

known as the OTC-assured temperature boundary (6).

$$T_{\min} \le T_{e_air} \le T_{\max} \quad (6)$$

D. The relationship between OTC-assured temperature boundary and VSHP power consumption

The thermal network of the experimental room can be utilized to calculate the energy needed to maintain the operative temperature in the OTC-assured boundary.

The equivalent network is a thermodynamic circuit; nonetheless, the dynamic behavior of the building model is ignored. The reason is that the presented approach in this work changes the temperature of a building in a range that, at all points, OTC is assured. In other words, in all temperature values between initial and steady-state values, the OTC is guaranteed, and HPs are exploited for handling network operational issues. Therefore, the steady-state response of the building is considered.

For example, the OTC-assured boundary is between 18°C and 21°C on a winter night. According to the step response (Fig.5), it takes 4000 sec. (nearly 1 hour) for the indoor air temperature to rise from 18°C to 21 °C and vice versa. If the DLC signal is applied an hour before the schedule (in the form of the day-ahead operational planning), then the temperature will be set at the intended value; therefore, the thermal behavior of the building between initial and steady-state values could be ignored.

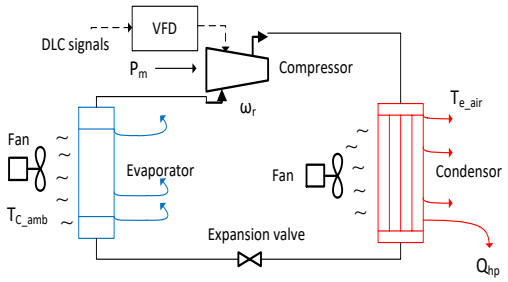


Fig. 6. Schematic diagram of a heat pump heating cycle.

E. Modeling of a DLC-enabled VSHP

Fig.6 shows that VSHP comprises an evaporator, a compressor, a condenser, and an expansion valve. The heating cycle of a heat pump extracts heat from the air outside, raises its temperature, and heats indoor air with warm air. Liquid refrigerant transforms into a gas by absorbing the outdoor air heat in the evaporator. The compressor raises the gas pressure and temperature. The hot gas passes through a condenser coil in the indoor space. Its temperature is higher than the indoor air temperature. Therefore, the gas transfers heat to the indoor space and condenses into a liquid. Eventually, the fluid passes through the expansion valve. The cycle terminates by lowering the liquid's pressure and temperature.

The shaft speed (ωr), condenser ambient temperature (TC-amb), and evaporator air temperature (Te-air) are the input variables for the VSHP model. Only ωr is controlled. Compressor mechanical power (Pm) and heat rate (Qhp) are the output variables. Additionally, the coefficient of performance (COP), which is defined as the ratio of Qhp to Pm, is used to assess the VSHP performance. The power usage of the fan is disregarded. Compression consumes the majority of the VSHP input power. VSHP has a dynamic behavior in response to the DLC signals; however, as stated earlier, the DLC signal was applied long enough before the instant of operation; therefore, in this work, a linear steady state function has been utilized for VSHP modeling (7).

$$P_m = k_\omega \omega_{r0} + k_C T_{C-amb0} + k_e T_{e-air0} + k_{offset} \quad (7)$$

In [31], multiple polynomial regressive algorithms were applied to 2210 different combinations of the input variables over typical VSHP operating points to find the coefficients kω, kC, ke, and koffset. Te-air0 is the indoor air temperature ensuring the OTC. It is determined by the PSO algorithm; Tc-amb0 is the outdoor air temperature and a known variable; therefore, the equation is deployed to find the speed ωr0 which is necessary for producing the mechanical power Pm. Subscript '0' denotes the parameter values at steady condition.

F. HPs minimum and maximum consumption calculation for winter

In this section Tideal, Tmin, and Tmax are employed to calculate the minimum and maximum HPs power consumption (Pmin and Pmax, respectively). In the following sections, Pmin and Pmax are utilized in the optimization procedure to

determine HPs flexibility in DRPs. Any value for HPs consumption between Pmin and Pmax determined by the PSO will satisfy the OTC.

In winter, if the outdoor temperature becomes lower than Tmin, then the minimum power consumption of the HPs is equal to the power needed for heating the temperature to Tmin. The maximum consumption of the HPs is the power for heating the temperature to Tideal. When the temperature is in other areas, the minimum and maximum consumption of HPs are determined using the Eq. (8).

$$P_{HP_{\max,\min}} \begin{cases} \begin{pmatrix} P_{\max} = P_{T_{ideal}} \\ P_{\min} = 0 \end{pmatrix} & T_{\min} \le T \le T_{ideal} \\ P_{\max} = P_{\min} = P_{T_{ideal}} & T \ge T_{ideal} \text{ or } T \ge T_{\max} \end{cases} \quad (8)$$

P_(T_ideal) is the power needed to maintain indoor air temperature at Tideal.

Temperature is a constant parameter; therefore, in [35], a 'voltage source' is considered the electrical equivalent of temperature. The current source is the electrical equivalent of HPs thermal power (Qhp). In the experimental room model (Fig.3), at a specific hour, for a definite value of ambient temperature ($T_{ambient}$), a certain value of Qhp is needed for heating the building to Tmin /Tideal. T_{e_air} (the indoor air temperature) is replaced by a voltage source with the value Tmin /Tideal. HPs power consumption for generating Qhp is determined using the COP. The index is supposed to be 0.7.

G. Test network

The chosen test network under examination is a modified IEEE 33-bus test system. The technical data of the network is provided in [43]. The modification includes a WT installation in bus no.18 and 20% of HPs penetration in each bus (Fig.7).

III. Uncertainty management of renewable generations using HPs

This work introduces a decision-making framework that exploits HPs and a WT reactive power generation capability to manage the uncertainty of wind power. Occupants' thermal comfort is assured consistently. PSO is employed to determine optimized decision variables.

A. Uncertainty Modeling

The general optimization problem is defined in (9) - (11), where a series of decision variables optimize the OF. Equality and inequality constraints will limit the optimized decision variables' values.

$$\min_{X} f(X, \bar{\psi}) \quad (9)$$

$$\mathbf{H}_{n}(\mathbf{X}, \bar{\psi}) \le 0, n \in \Gamma_{ineq} \quad (10)$$

$$\mathbf{G}_{\mathbf{m}}(\mathbf{X}, \bar{\psi}) = 0, m \in \Gamma_{eq} \quad (11)$$

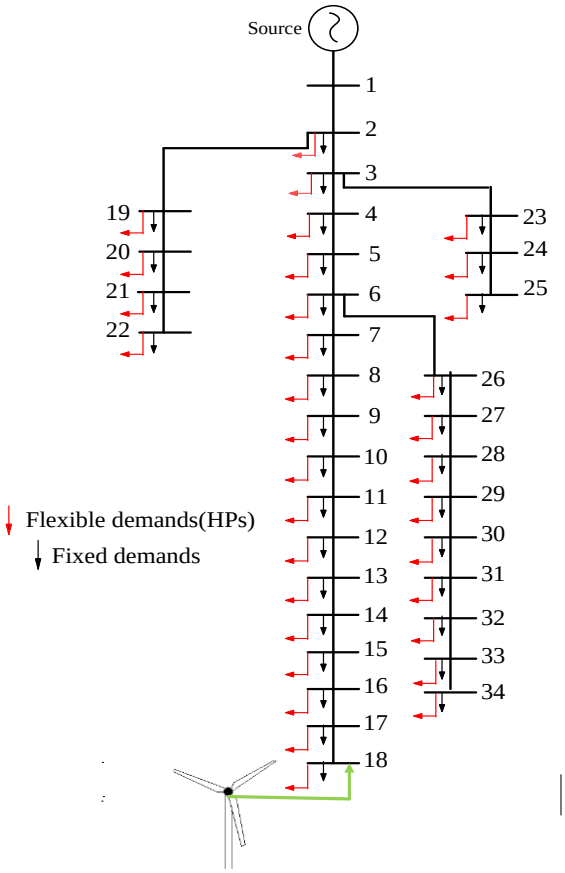


Fig7.Modified IEEE 33-bus test system.

X is the vector of decision variables, $\bar{\psi}$ is the predicted value of the uncertain parameter, Γ is the set of all constraints, H and G are the set of inequalities and equalities for the variables X.

B. IGDT Risk Averse (RA) strategy

If the OF is optimized based on $\bar{\psi}$, then underestimation of the wind forecast will deteriorate the OF from the optimized value. In this case, the DSO, as the decision maker, specifies the maximum tolerable deterioration in the optimized value of the OF(15). In return, IGDT determines X and the maximum manageable underestimation of wind forecast ($\hat{\alpha}$ in (12)). If the DSO operates the network based on the vector X, then for the uncertainty gap between zero and $\hat{\alpha}$, the value of the OF is restricted to the DSO pre-specified critical limitation (15) and all constraint equations remain true ((13) and (14)). IGDT Risk Averse (RA) strategy is formulated as:

$$\max_{\mathbf{X}} \hat{\alpha}(\mathbf{X}, \psi) \quad (12)$$

$$\mathbf{H}_{n}(\mathbf{X}, \psi) \le 0, n \in \Gamma_{ineq} \quad (13)$$

$$\mathbf{G}_{\mathbf{m}}(\mathbf{X}, \psi) = 0, m \in \Gamma_{eq} \quad (14)$$

$$\hat{\alpha} = \left\{ \max \alpha \mid \mathrm{f}(\mathbf{X}, \psi) \le \Lambda_{C} = (1+\beta_{c})\mathrm{f}_{b} \right\} \quad (15)$$

$$\psi \in \mathrm{U}(\bar{\psi}, \alpha) = \left| \frac{\psi - \bar{\psi}}{\bar{\psi}} \right| \le \alpha \quad (16)$$

C. IGDT Risk Seeker (RS) strategy

Overestimation of the wind forecast will improve the value of the OF. IGDT in the RS approach calculates a minimum value for the radius of uncertainty (17) that leads to a pre-defined improvement of the OF (20).

$$\min_{\mathbf{X}} \hat{\alpha}(\mathbf{X}, \psi) \tag{17}$$

$$\mathbf{H}_{n}(\mathbf{X}, \psi) \le 0, n \in \Gamma_{ineq} \tag{18}$$

$$\mathbf{G}_{m}(\mathbf{X}, \psi) = 0, m \in \Gamma_{eq} \tag{19}$$

$$\hat{\alpha} = \left\{ \min \alpha \mid f(\mathbf{X}, \psi) \le \Lambda_{O} = (1 - \beta_{O}) f_{b} \right\} \tag{20}$$

$$\psi \in U(\overline{\psi}, \alpha) = \left| \frac{\psi - \overline{\psi}}{\overline{\psi}} \right| \le \alpha \tag{21}$$

Λ_O as a pre-defined opportunistic limit, is hoped to be achieved when the realized values are the improved version of the forecasted ones. The expected level of the OF improvement is βo. The minimum value of α is which should be determined, while the value of the OF is kept below the parameter Λ_O.

D. Decision variables

Decision variables include HPs consumption in each bus.

E. Optimization procedure

The objective of an optimization problem is to identify a variable represented by a vector X=[x1,x2,x3,...xn] that minimizes or maximizes a cost function known as the fitness function or the objective function. The position vector, X, is an n-dimensional variable vector where n is the total number of variables in the problem. The OF evaluates the quality of a specific position vector X. Particle Swarm Optimization (PSO) is a metaheuristic optimization technique that solves challenging optimization problems with high efficiency and simplicity. However, several PSO variations exist because the performance of the normal PSO is prone to be caught in local extrema. Fuzzy logic concepts have widely improved the PSO algorithm. In this study, the performance of a modified version of PSO algorithms known as Adaptive Particularly Tunable Fuzzy Particle Swarm Optimization (APT-FPSO) is compared with the performance of the standard PSO. The standard PSO compares the outputs of this work's presented scenarios. Section 5 demonstrates that APT-FPSO produces more acceptable results than the standard PSO. In [38], PSO and in [39], APT-PSO optimization methods are, respectively, introduced. The standard PSO compares the outputs of this work's presented scenarios. Section 5 demonstrates that APT-FPSO produces more acceptable results than the standard PSO. In [38], PSO and in [39], APT-PSO optimization methods are, respectively, introduced.

PSO for each iteration generates a swarm of P position vectors (X). The velocity vector (V) moves the position vector from one iteration to the other one (toward a more optimal version).

$$\mathbf{X}_{i}^{t+1} = \mathbf{X}_{i}^{t} + \mathbf{V}_{i}^{t+1} \tag{22}$$

Identification: Uses the previous solutions, determines the best solution of a specific region.

Diversification: Looks for novel solutions and identifies areas that may have the solutions.

$$V_{i}^{t+1} = wV_{i}^{t} + c_{1}r_{1}\left(pbest_{i}^{t} - X_{i}^{t}\right) + c_{2}r_{2}\left(gbest^{t} - X_{i}^{t}\right) \tag{23}$$

Inertia: Makes particles move in the same direction and at the same speed.

Personal influence: Improves the individual. Using the previous position

Social influence: Makes the particle follow the best neighbors' direction

The parameter w is the inertia weight with a positive constant. The parameter balances the global and local searches. The first search is known as exploration, and the second search is known as exploitation. Higher values of w dominate exploration; however, lower values of the parameter dominate exploitation. $pbest_i^t$ is the personal best record of the ith particle in the t^{th} iteration, and $gbest^t$ is the global best in the tth iteration; r_1 and r_2 are random numbers within the range [0; 1]; c_1 and c_2 and are constants known as the personal and global learning coefficients, respectively.

F. The developed adaptive particularly tunable fuzzy PSO algorithm

As already mentioned, the standard PSO variants have facilitated the algorithm from premature convergence phenomena. The main objective of PSO variants is to achieve an adaptive, dynamic, well-balanced strategy for adjusting PSO's setting parameters during exploration and exploitation. Fuzzy Adaptive algorithms are more useful than other variants of the PSO. They utilize fuzzy logic concepts to tune the setting parameters of the PSO algorithm adaptively and dynamically. The Adaptive Particularly Tunable Fuzzy Particle Swarm Optimization (APT-FPSO) proposes the best strategy for balancing between exploration and exploitation [46]. Section IV demonstrates that APT-FPSO produces more acceptable results than the standard PSO. In [44], PSO and in [45], APT-PSO optimization methods are, respectively, introduced. The standard PSO compares the outputs of this work's presented scenarios.

The Mamdani fuzzy inference system (FIS) has two inputs. The first input normalizes the iterations (NIt) from the start (NIt = 0) to the end (NIt = 1) of the algorithm. Eq. (24) represents the normalized iterations.

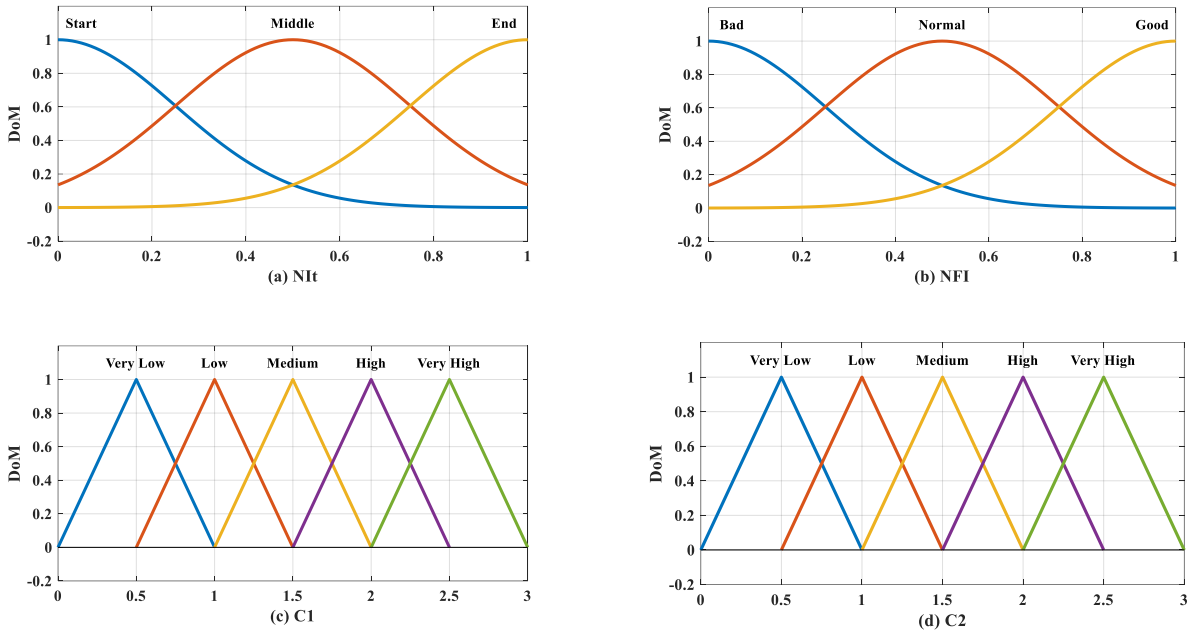
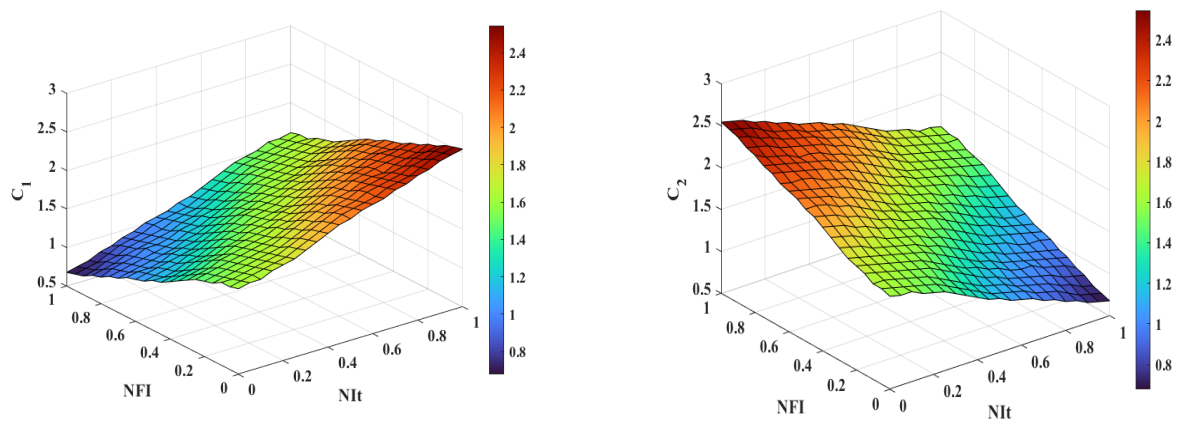


Fig.8 Membership functions of inputs (a, b) and outputs (c, d) of the developed FIS



(a) (b)

Fig9. Surfaces of the inputs and the outputs for the rule-base structure No.1.

$$NIt = \frac{\text{Current iteration}}{\text{Maximum number of iterations}} \quad (24)$$

Three linguistic variables "Low", "Medium", and "High" and corresponding three Gaussian Membership Functions (MFs) fuzzify the normalized iterations. The second input of the developed FIS is the fitness value of each particle. The APT-FPSO algorithm uses the best and worst swarm fitness values at each iteration to normalize particle fitness. (25) formulates the normalized fitness index (NFI).

$$NFI = \frac{fitness_{t,i} - \min(fitness_t)}{\max(fitness_t) - \min(fitness_t)} \quad (25)$$

$fitness_{t,i}$ is the fitness value of the i^{th} particle in the t^{th} iteration. The $\max(fitness_t)$ and $\min(fitness_t)$ are the maximum and minimum fitness values of the swarm in the t^{th} iteration, respectively. Three Gaussian MFs are the second input NIt linguistically called low, medium, and high. Fig. 8 (a) and Fig.8 (b) indicate the inputs of the developed FIS. The outputs of the proposed FIS are personal and global learning coefficients, i.e., $c_{1,t}^{i}$ and $c_{2,t}^{i}$. Their values are proved to be within the range [0.5, 2.5] in [41, 42]. $c_{1,t}^{i}$ and $c_{2,t}^{i}$ are the learning coefficients of c_1 and c_2 for the i^{th} particle in the t^{th} iteration respectively. Five triangular MFs represent the outputs of the developed FIS known as, very low, low, medium, high, and very high ($c_{1,t}^{i}$ and $c_{2,t}^{i}$). Briefly, the developed FIS

has normalized iteration and normalized fitness index as the inputs, and two outputs known as $c_{1,t}^{i}$ and $c_{2,t}^{i}$.

The outputs of the algorithm are shown in Fig.8(c) and Fig.8(d) For the proposed inputs and outputs, many rule bases can be introduced with unique performances. The rule-base surfaces utilized by this work are shown in Fig.9.

G. Objective function

In this work, the OF is formulated as:

$$f(X, W_T, \beta) = k_1 \left| \sum_{n=2}^{33} \left(\frac{P_{HPs,n}}{P_{DR0,n}} \right) \right| + k_2 W_T + G \quad (26)$$

$P_{HPs,n}$ is the optimized consumption of HPs in bus No.n. $P_{DR0,n}$ shows the consumption of the loads when HPs offer no flexibility in bus No.n. G is a penalty factor which is a linear summation of constraints. PSO minimizes both terms in (26). The PSO utilizes HPs DRPs participation minimizing the first term. The second term is the IGDT OF and is defined as follows:

$$W_T = (1-\alpha)\overline{W}_T \quad (27)$$

$$W_T = (1+\alpha)\overline{W}_T \quad (28)$$

In RA and RS strategies, WT, as the realized value of the uncertain parameter, is related to the forecasted value by (27) and (28). $\overline{W}_T$ is the wind power predicted value.

H. Constraints

• *IGDT constraints*: Critical and opportunistic values of CI are utilized as the DSO or the decision maker inputs to the IGDT-based PSO algorithm ((29) and (30)).

$$\Lambda_C = CI_c = (1+\beta)CI = (1+\beta)\sum_{L=1}^{32} S_L \quad (29)$$

$$\Lambda_O = CI_O = (1-\beta)CI = (1-\beta)\sum_{L=1}^{32} S_L \quad (30)$$

• The power flow constraint: The power flow equation ensures that the power which the network and the WT provide (P_{net} and P_{WT}, respectively) is equal to the summation of HPs consumption (P_{HPs}) and the network power loss (P_{loss}).

$$P_{net} + P_{WT} = P_{HPs} + P_{loss} \quad (31)$$

• The operating limits of WT, HPs and bus voltages: The OTC-assured operating limit of HPs is (32). Safe operating limit for bus voltages is formulated in (33).

$$P_{min} \le P_{HPs} \le P_{max} \quad (32)$$

$$0.9\,pu \le V_{busj} \le 1.1\,pu \quad (33)$$

I. The role of heat pumps in uncertainty management

The decision maker (DSO) defines specific values for the indices Λc, Λo, or β. Moreover, the limitations denoted in section 4.9.2, are inequality constraints of the optimization algorithm (the flowchart in Appendix A). The OF optimizes HPs consumption and the radius of uncertainty(α) simultaneously. Sections 4.9.2 and 4.9.3 prove that placing the term related to HPs consumption along with the one related to the IGDT will improve the output of the theory in both RA and RS strategies

J. RA strategy

For each iteration of the PSO, after determining the population, the Congestion Index (CI) is calculated by carrying out power flow while the constraint provided by the IGDT is examined (34).

$$CI < \Lambda_C or \Lambda_O \quad (34)$$

Candidate solutions with α closer to 1 are more liable to be selected as the final solution; according to (27), the network and the DSO will be protected against losing a higher portion of the WT generation. The higher value of α̂ corresponds to the lower value of the WT generation (27) and a higher value of CI. Because of the IGDT constraint (34), candidate solutions with α closer to 1 may not be the final solution. Therefore, the only obstacle to achieving values is the limitation provided by the IGDT. Placing the sentence related to the optimization of the HPs consumption in the OF and trying to reduce their consumption is an attempt to reduce the CI and achieve the PSO to populations with α closer to 1.

K. RS strategy

Candidate solutions with $\check{\alpha}$ closer to 0 are more liable to be selected as the final solution; according to (28), the amount of improvement desired by the DSO will occur for a lower increase in the WT generation. Therefore, the decision-maker can be more hopeful of realizing his optimism about the WT generation increase and the improvement defined in the CI. Reducing the consumption of HPs can have the same effect as increasing the generation of the WT on the CI. Therefore, the desired improvement will be achieved with a lower increase in WT generation.

IV. Simulation results and discussion

In section *A* and *B* conservative and opportunistic approaches have been taken into consideration, respectively. For every single case, the outputs are compared for two scenarios:

• **Scenario I (user-defined)**. Occupants' pre-defined favorite temperature boundary is utilized for HPs consumption determination. The temperature is assumed to be 28 ℃ for winter and 18 ℃ for summer. Based on the typical wear of occupants in winter it is assumed that occupants intrinsically introduce temperatures which are equal to PMV +2 for winter and -2 for summer (Table.1).

• **Scenario II (DSO-defined)**. In this scenario which has been proposed by this paper, instead of using occupants' personal view of the suitable temperature range (which is the most common way of HPs DRPs participation), ASHRAE55

is exploited to find the real thermal needs and the appropriate boundary for occupants. Consequently, the utmost HPs degree of flexibility will be achievable in DRPs.

A. Conservative approach

The first group of simulations are performed in a case in

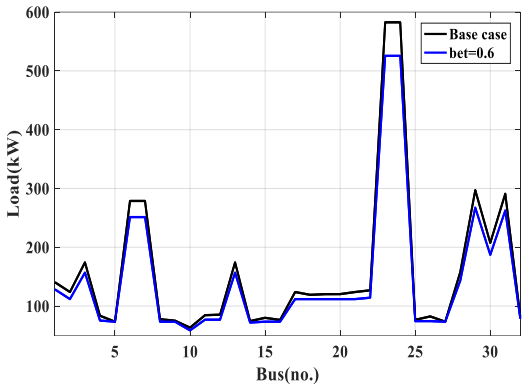


Fig.10. Scenario I HPs consumption alteration versus the base case.

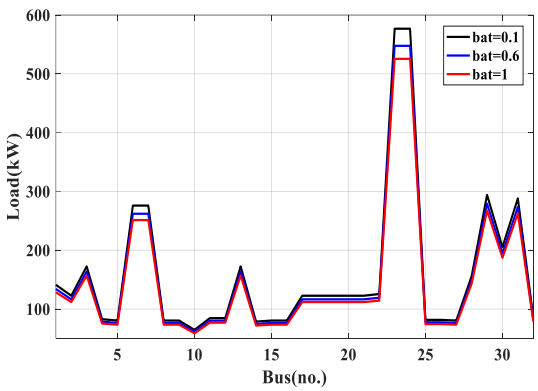


Fig.11. Scenario I HPs consumption alteration versus β.

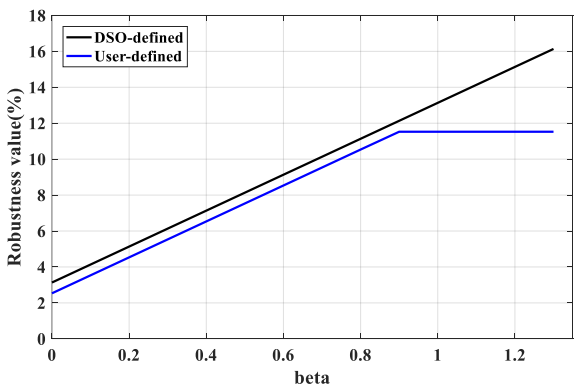


Fig.12. Radius of uncertainty.

which underestimation of the wind forecast is of interest. Thus, the WT will generate less than what is expected (27). A 'base case study' is considered in which no uncertainty exists in the WT power generation. The results of HPs consumption optimization by PSO can be seen in Fig.10.

As can be seen, the loads consumption related to a specific level of critical congestion index (β=0.6) is less than the base case. DSO has decreased the loads opportunity for increasing $\alpha\hat{}$ to a higher value. As the β value rises, the power consumption has been set to lower values (Fig.11), and consequently the value of $\alpha\hat{}$ will be raised (Fig.12).

Contrary to [28] in which a fixed predefined value of load flexibility is assigned to a bus with the most influence on

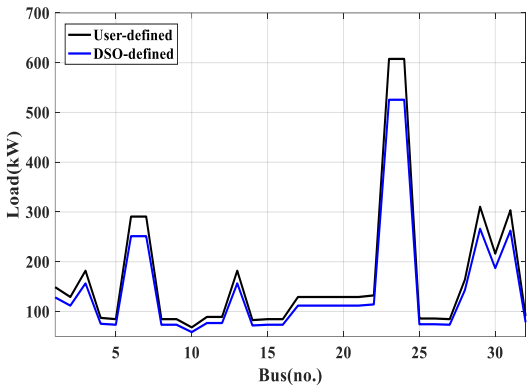


Fig.13. Scenario I & scenario II HPs consumption alteration for β=0.6

the OF, in this work, a more realistic situation is taken into consideration for HPs flexibility. Accordingly, HPs are distributed all over a practical distribution system; therefore, HPs in each bus are considered to provide flexibility for uncertainty management. Moreover, HPs in each bus are considered to offer a different level of flexibility in a way that buses with higher penetration of HPs offer higher levels of flexibility; therefore, without violating the OTC, peak shaving has been performed by β increment and the proposed operating point (set of decision variables) would be more attractive for the DSO to be selected.

a. Scenarios comparison from uncertainty management point of view

Two proposed scenarios have approximately the same reaction to β increment; but, for a definite value of β, scenario II determines a lower consumption for HPs (Fig.13). Fig.13 depicts the results for β=0.6 but the same results can be obtained for other values of β. Fig.12 compares $\alpha\hat{}$ for both scenarios. In fact, higher values of α and a wider range of possible increase for β, are defined by Scenario II ($0.1\leq \beta\leq 0.9$ for the scenario I and $0.1\leq \beta\leq 1.4$ for scenario I). For β values higher than 0.9, HPs consumption in scenario I remain constant (PHPs=Pmin or Pmax in Appendix A). It means HPs' consumption will no longer be the decision variable or be effective in uncertainty management. Higher values for β in scenario II mean more effective usage of HPs in uncertainty regulation. Therefore, from an uncertainty management point of view, scenario II would lead to higher levels of wind forecast underestimation (29) and more acceptable results.

b. WT power reduction capability

In the conservative approach, the realized values of WT power generation are lower than the forecasted ones. For a specific value of ΛC 'dispatchable DG output' refers to the minimum value of WT power generation which can be accommodated by the network. Therefore, in the proposed method, wider WT power generation variations are allowed which are more appropriate from a conservative approach perspective (Fig.14).

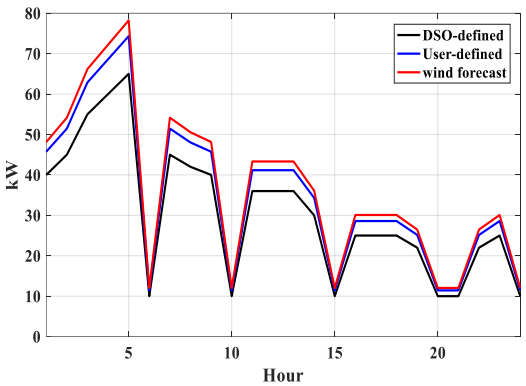


Fig.14. Scenarios WT manageable WT power generation with critical limit ΛC=0.7

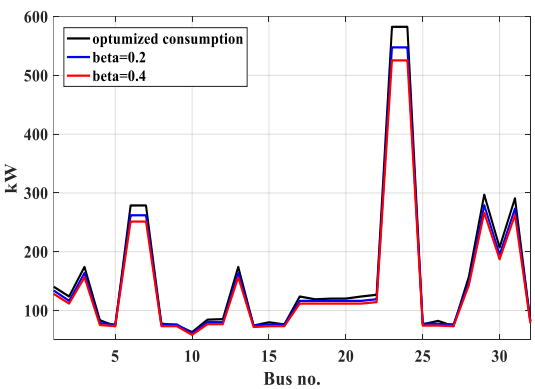


Fig.15. Scenario I HPs consumption vs. β increment (opportunistic approach).

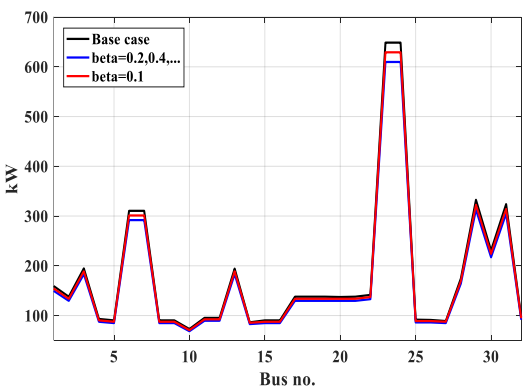


Fig.16.Scenario II HPs consumption vs. β increment (opportunistic approach).

B. *Opportunistic approach*

In the test system, if the wind power goes higher than the predicted value, then the congestion index will decrease. In the proposed scenarios, higher values of β are accompanied by lower values of HPs consumption (Fig.15 and Fig.16). According to (30) increasing the β value leads to CI index improvement. Moreover, in comparison with the conservative approach, β could not grow higher than 0.4 (40% improvement in the OF). This is

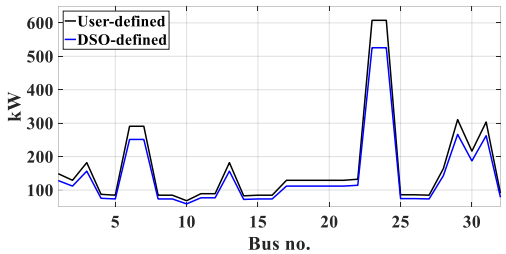


Fig.17. Scenario I & scenario II HPs consumption (β=0.6, opportunistic approach)

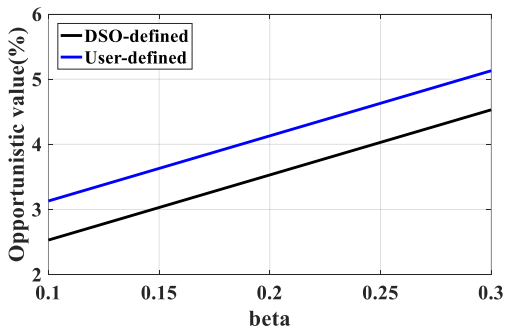


Fig.18. Scenario I scenario II radius of uncertainty.

because of the fact that the WT generation increment could only provide a limited improvement and would never cause the opportunistic congestion index to lower values.

a. Scenarios comparison from uncertainty management point of view

Fig.17 and Fig.18 compare HPs consumption and radius of uncertainty for both scenarios, respectively. Scenario II offers lower values for HPs consumption and $\hat{\alpha}$. Therefore, from the uncertainty management point of view, scenario II would lead to more acceptable results because, with lower HPs consumption, a lower wind power generation increment is required to produce the same enhancement in the CI parameter.

b. WT power generation for opportunistic scenario

For a specific value of ΛO, "opportunistic WT power generation" refers to the minimum value of WT power generation increment which is needed to meet the DSO predefined congestion index while all constraints are met. As can be seen in Fig.19, the proposed method assigns lower values for opportunistic WT power generation which are more desirable.

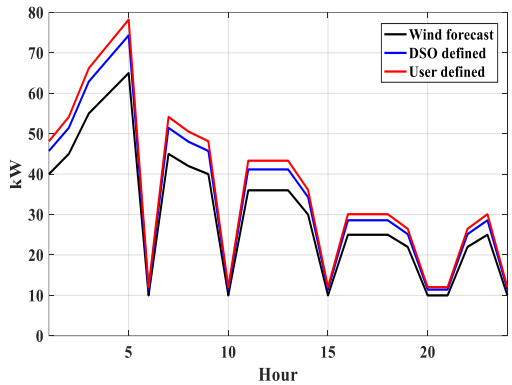


Fig.19. Scenarios WT opportunistic WT power generation with opportunistic limit Λ_O=0.1.

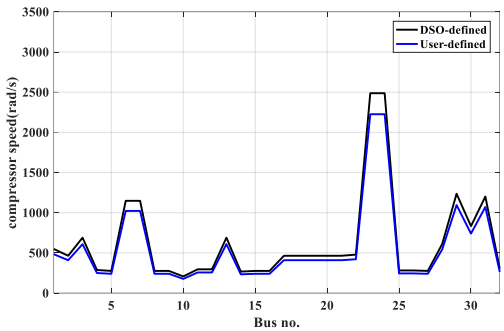


Fig.20. Scenario I and scenario II compressor speed

C. *Technical and operational comparison*

To show the technical superiority of scenario II, a number of parameters that are effective in the operation of equipment and network have been examined for a conservative approach.

a. Compressor speed

As it was stated earlier, A VFD which is driven by DLC signals controls the compressor speed. So, power consumption of HPs is controlled by the speed adjustment. Lower VSHPs power consumption in scenario II means that the VFD drives compressor at lower speed which reduces the wear in the mechanical components. Fig.20 compares compressor speed variations between two scenarios.

b. Compressor Coefficient of Performance

As was stated in section 2.4, COP can be calculated by (35).

$$COP = \frac{Q_{hp}}{P_m} \tag{35}$$

The larger the COP, means that a fixed amount of Pm produce higher thermal energy. In other words, less mechanical power is required to produce a certain amount of thermal energy. Therefore, higher COP, higher efficiency, lower energy (power) consumption and thus lower operating costs are the results of the proposed method (Fig.21).

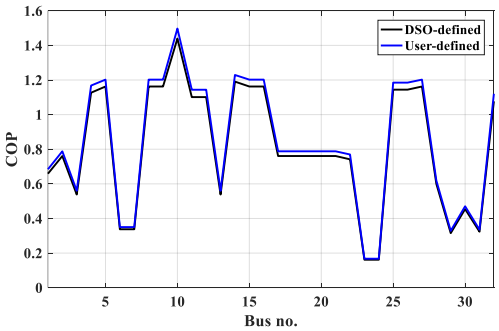


Fig.21. Scenario I & scenario II COP.

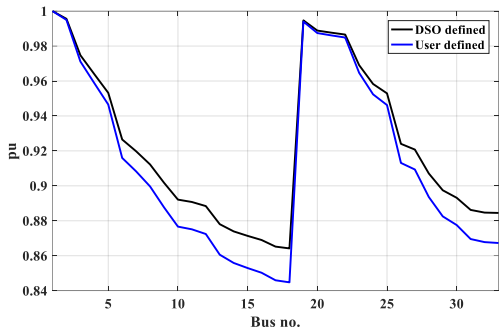


Fig.22. Scenario I and scenario II voltage profile.

c. Voltage profile

For β=0.1, the voltage profiles are examined for two scenarios. In the proposed method, due to lower HPs consumption, the voltage profile is improved across the network. As can be seen in Fig.22, it is obvious that buses 13-18 and 29-33 have the lowest voltage magnitude.

D. *PSO and APT-FPSO results comparison*

Applying the APT-FPSO optimization method to both risk-seeker and risk-averse strategies can improve some results. In terms of radius of uncertainty, this optimization method will produce the same results in both strategies. But the amount of consumption in the network will be reduced to an acceptable level due to the use of the APT-FPSO method. In the following, these two optimization methods will be compared for two risk-seeker and risk-averse strategies for scenario II.

a. Risk-averse strategy

In Fig.23, the test system power consumption is compared for β=0.2. Although the APT-FPSO strategy has slightly increased the consumption in some buses, in total, by using this method the amount of consumption in the entire network has decreased by 176 kW. This amount is 20 kilowatts more than the typical consumption in bus bar No. 32 of the IEEE 33-bus network.

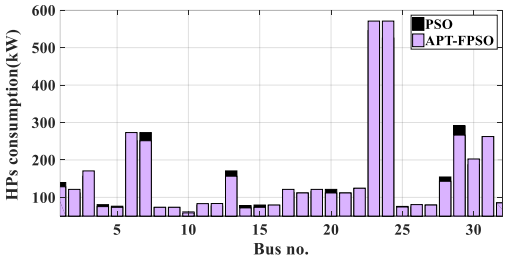


Fig. 23. PSO and APT-FPSO HPs consumption for RA strategy.

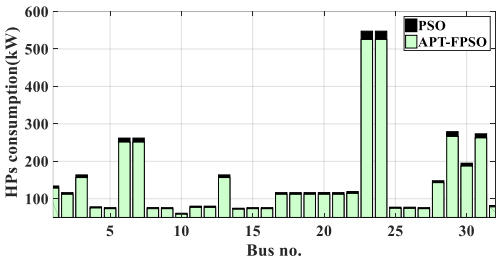


Fig.24. PSO and APT-FPSO HPs consumption for RS strategy.

b. Risk-seeker strategy

In Fig.24, the amount of network power consumption per bus is compared for b=0.2 and using two optimization methods. The APT-FPSO strategy has reduced the consumption in all buses and, the total amount of consumption reduction is 200 kilowatts, which is equivalent to the typical consumption in bus No. 33 of the IEEE 33-bus network.

V. Conclusion

To simultaneously achieve two main aims, a framework based on the ASHRAE55 standard for determining the optimal flexibility of HPs in DRPs has been proposed. To achieve the first goal means guaranteeing the OTC, a new method to control the consumption of HPs was presented. In the first step, the ASHRAE55 standard determines the temperature ranges in which the OTC is assured during the day. Then, using the electro-thermal network of the experimental room at MIT, the boundary of thermal energy required to stabilize the room temperature in the abovementioned ranges and the corresponding HPs power consumption boundaries were determined. The results of using this method were compared with the common one in which the temperature of the building is adjusted within the predetermined limits by the residents. The method has been proposed by this work reduces the consumption of HPs by an average of 13%. To achieve the second goal means managing the uncertainty of the WT, The DSO handles this uncertainty by controlling the power consumption of HPs. The effectiveness of two methods of controlling the consumption of HPs in managing uncertainty is compared using two risk-averse and risk-seeker strategies provided by the IGDT. Using the proposed method, in the first strategy, the radius of uncertainty increases by an average of 6%, and in the second strategy, it decreases by an average of 5.5%. The proposed method results are also more acceptable for network voltage profile and compressor mechanical wear.

A. Future works

• Uncertainty management using IGDT by coordinated operation of energy storage and HPs while considering OTC as a constraint can be an attractive topic for future research.

• To further convince the DSO and HPs owners to adopt the proposed scenario, the environmental and economic objectives could be considered in the optimization problem which can be considered as future work.

• To determine a complete framework for HPs participation in DRPs using classical and fuzzy approaches to find the superior one is also an attractive topic that can be investigated in future work.

REFERENCES

[1] The Paris Agreement [Online]. https://unfccc.int/process-and-meetings/the-paris-agreement/the-paris-agreement.

[2] Lingxi, Z., Chapman, N., et al.:' Exploiting electric heat pump flexibility for renewable generation matching'. Int. Conf. IEEE Manchester Power Tech, Manchester, UK, June 2017; pp.1-6. lingxi.zhang@manchester.ac.uk

[3] Residential Energy Consumption Survey (RECS) [Online].https://www.eia.gov/consumption/residential/reports/2015/overview

[4] Baldib, S., Korkasa, C., et al.: 'Automating occupant-building interaction via smart zoning of thermostatic loads A switched self-tuning approach', Appl. Energy,vol. 231, pp. 1246–1258, 2018

[5] Korkas, C., Baldi S., et al.:' Occupancy-based demand response and thermal comfort optimization in micro grids with renewable energy sources and energy storage', Appl. Energy, vol. 163, pp. 93–104, 2016

[6] Anand, P., Sekhar,C., Cheong D., et al.:' Occupancy-based zone-level VAV system control implications on thermal comfort, ventilation, indoor air quality and building energy efficiency', Appl. Energy ,vol. 204, pp. 1–14, 2019

[7] Diekerh, M., Peterssen F.:' Hierarchical distributed robust optimization for demand Response Services', IEEE Trans. smart grid ,vol. 9, pp. 6018-6029,2018.

[8] Angelis,F., Boaro, M., et al.:' Optimal home energy management under dynamic electrical and thermal constraints', IEEE Trans. Industr. Inform., 2013, 9, (3), pp.1518-1527 vol. 9, pp. 1518-1527, 2013.

[9] Marco,Pau., Jochem, C.:' Impact of customers flexibility in heat pumps scheduling for demand side management'. IEEE.Int. Conf. on Environment and Electrical Engineering, Milan, Italy, pp.1-6, 2017.

[10] Khatibi, M., Bendtsen, J., et al.:' Exploiting Power-to-Heat Assets in District Heating Networks to Regulate Electric Power Network'. IEEE Trans. Smart Grid, vol. 12, no. 3, pp.2048-2059, 2021.

[11] Csetvei, Z., Ostergaard, J., Nyeng P.:' Controlling price responsive heat pumps for overload elimination in distribution systems', 2nd IEEE PES Int. Conf. and exhibition on Innovative Smart Grid Technologies,

Manchester, UK, Dec 2011, pp.1-8 vol. ---, no. ---, pp.1-8, 2011.
[12] Mendaza, C., Szczesny, I., et al.:'Demand Response Control in Low Voltage Grids for Technical and Commercial Aggregation Services', IEEE Trans. Smart Grid vol. 7, no. 6, pp.2771-2780, 2016.
[13] Pedersen, T., Nielsen, K. Andersen, P:' Maximizing Storage Flexibility in an Aggregated Heat Pump Portfolio', IEEE Conf. on Control Applications, Juan Les Antibes, France, pp.1-6, 2014.
[14] Ponci,F., M., Monti, A.:' Optimal scheduling of heat pumps for power peak shaving and customers thermal comfort', Int. Conf. EEEIC/ I& CPS Europe, Palermo, Italy,pp.23-34, 2018.
[15] Kim, Y., Norford, L.K., Kirtley J.L.:' Modeling and analysis of a variable speed heat pump for frequency regulation through direct load control', IEEE Trans. Power Syst.,vol. 30, no.1, pp.397-408,2015.
[16] Kazemi-Razi M., Abyaneh H. a, Nafisi H. a, Ali Z. b, Marzband M.:' Enhancement of flexibility in multi-energy microgrids considering voltage and congestion improvement: Robust thermal comfort against reserve calls', sustainable cities and society, vol.74, pp.1-13, 2021.
[17] Jadidoleslam M., and Ghaseminezhad M.:' Reliability-based probabilistic wind power planning considering correlation of load and wind', Industrial electronics control and optimization,vol.5, no. 4, pp.305-315, 2022.
[18] Malekijavan A., Aslinezhad M., and Zaferani H.' Reliability-Based Operation in Energy Hubs with Several Energy Networks', Industrial electronics control and optimization, vol.4, no. 4, pp.433-444, 2021.
[19] Shirmardi A., Joorabian M., and Barati H.' Green Micro-Grid Operation Constrained to Reliability and Flexibility Indices in the Presence of Distributed Generations and Energy Storage Systems', Industrial electronics control and optimization, 2021,4, (4), pp. 397-407. vol. 4, no. 4, pp.397-407, 2021.
[20] Vosoogh M., Rashidinejad M., Abdollahi A., and Ghaseminezhad M.' Efficient networked microgrid management considering plug-in electric vehicles and storage units', Industrial electronics control and optimization,vol. 4, no. 2, pp.245-255,2021.
[21] Haiyan X., Yuqing C. et al.:' A new multi-timescale optimal scheduling model considering wind power uncertainty and demand response', International journal of electrical power and energy systems, vol. 147, pp.1-11, 2023.
[22] Linjun Z, Jiazhu X et al.:' Day-ahead interval optimization for CCHP system considering uncertainty of wind power and PV', International journal of electrical power and energy systems, 2022, 138: pp.1-9. vol.138,pp.1-9, 2022.
[23] Ding, Guo, Qiannan, and Jermsittiparsert, Lekvan et al.:' Economic and environmental assessment of multi-energy microgrids under a hybrid optimization technique', sustainable cities and society,vol. 65, pp.1-12, 2021.
[24] Coelho A. Neyestani N. et al.:' Wind variability mitigation using multi-energy systems', Electrical power and energy system, vol. 118, no. pp.1-9, 2020.
[25] Correa C.A, Michiorri A., Kariniotakis G.:' Optimal Participation of Residential Aggregators in Energy and Local Flexibility Markets', IEEE Trans. on smart grid, vol. 11, no. 2, pp.1644-1656, 2020.
[26] Yakov Ben-Haim, "Information Gap Decision Theory," The Technion Haifa, Israel, Feb, 2006
[27] A. Dolatabadi, M. Jadidbonab and B. Mohammadi-ivatloo, "short-term scheduling strategy for wind-based energy hub: a hybrid stochastic/IGDT approach," IEEE Trans. Sustainable Energy, vol. 10, no. 1, pp. 438–448, 2019.
[28] C. Murphy,Soroudi.A and A.Keane, "Information Gap Decision Theory-based congestion and voltage management in the Presence of uncertain wind power," IEEE Trans. Sustainable Energy, vol. 7, no. 2, pp. 841–849, Nov. 2015.
[29] P.Li, Z.Wang, et al. "Two-stage optimal operation of integrated energy system considering multiple uncertainties and integrated demand response," Energy, vol. 225, pp. 1–12, Jun. 2021.
[30] A. Kazemdehdashti , M. Mohammadi , A.R. Seifi , M. Rastegar. "Stochastic energy management in multi-carrier residential energy systems," Energy, vol. 225, pp. 1–12, May. 2020.
[31] X.Jina,b, J.Wua,Y.Mu, et al. "Hierarchical microgrid energy management in an office building," Appl.Energy, vol. 208, pp. 480–494, Oct. 2017.
[32] X.Jina,b, J.Wua,Y.Mu, et al. "Resilient configuration approach of integrated community energy system considering integrated demand response under uncertainty," IEEE Access, vol. 7, pp. 87513 - 87533, Jun. 2019.
[33] I. Ballarini, S.P. Corgnati, V. Corrado,' Use of reference buildings to assess the energy saving potentials of the residential building stock: The experience of TABULA project', Energy Policy 68 vol. 68, pp.273-284, 2014.
[34] Zakula T, 'Model predictive control for energy efficient cooling and dehumidification,' Dept. Arch Massachusetts Inst. Technol, Massachusetts, Ph.D. thesis (2013).
[35] Kim Y, Norford LK, Kirtley JL, 'Modeling and analysis of a variable speed heat pump for frequency regulation through direct load control,' IEEE Trans Power, vol. 30,no.1, pp.397–408, 2015.
[36] Evelyn Sperber, Ulrich Frey, Valentin Bertsch,' Reduced-order models for assessing demand response with heat pumps -insights from the German energy system', Energy & Buildings,vol. 223-,pp.1-18, May 2020.
[37] ANSI/ASHRAE Standard 55-2004: 2004.
[38] 2020 ASHRAE Handbook—HVAC Systems and Equipment',https://ashrae.org/technicalresources/ASHRAE-handbook/description-2020.
[39] ISIRI 14384 1st. Edition: 2011
[40] Zhongping Lina, Shiming Deng,' A study on the thermal comfort in sleeping environments in the subtropics—Measuring the total insulation values for the bedding', Building and Environment, 2008,43, pp.905-916. vol.43, pp.905-916, 2008.
[41] Iran's Provinces annual average of total monthly solar radiation[Online].https://www.researchgate.net/figure/Irans-Provinces-annual-average-of-total-monthly-solar-radiation
[42]Climatein Tehran [Online]. https://www.worlddata.info/asia.
[43] Line data of the IEEE 33-bus radial distribution system [Online]. https://www.researchgate.net/figure/Line-data-of-the-IEEE-33-bus-radial-distribution-system.
[44] Koohi, Iraj:' Optimizing Particle Swarm Optimization algorithm', IEEE 27th Canadian Conf. Electrical and Computer Engineering, (CCECE), Toronto, Canada, May 2014.
[45] N. Bakhshinezhad, S.A. Mir Mohammad Sadeghi, et al.:' Adaptive particularly tunable fuzzy particle swarm optimization algorithm', Iranian Journal of Fuzzy Systems, vol. 17, no. 1, pp. 65–75, 2020. vol.17, no. 1, pp. 65-75, 2020.
[46] P. Melin, "Optimal design of fuzzy classification systems

using PSO with dynamic parameter adaptation through fuzzy logic", Expert Systems with Applications,vol. 40, no.8-, pp.3196-3206,2013.
[47] A. P. Engelbrecht, Fundamentals of computational swarm intelligence, John Wiley & Sons, 2005.



Mohammadmehdi Sedaghatzadeh was born in Iran, in 1980. He is a PhD student in power engineering at Department of Electrical and Electronics Engineering, Shiraz University of Technology, Shiraz, Iran. He received his M.S. degree in Electrical Power Engineering from the Islamic Azad University, Saveh, Iran, in 2007. He received the B.S. degree in electronics engineering from Islamic Azad University, Tehran, in 2002. He is an expert in electrical engineering in National Iranian South Oil Company. His research interests include smart grid, Micro-grid demand side management, and renewable generation.



Mohsen Gitizadeh was born in Iran, in February 1976. He received the B.S. degree in electrical engineering from Shiraz University, Shiraz, Iran, in 1999, and the M.S. and Ph.D. degrees from the Iran University of Science and Technology, in 2001 and 2009, respectively. He is currently a Professor with the Department of Electrical and Electronics Engineering, Shiraz University of Technology, Shiraz. His current research interests include power system operation and control, voltage stability, optimization, demand side management, and FACTS devices.



Saeed Hasanvand received his BSc. degree from Shahid Chamran University of Ahvaz, Iran, in 2009, the MSc. degree from University of Isfahan, Iran, in 2012, and the PhD. from Shiraz University of Technology, Iran, in 2017. He is currently an assistant professor in electrical engineering at Firouzabad Institute of Higher Education. His research interests include power system stability and optimization, micro-grids, renewable energies, FACTS devices, and power system reliability.

Appendix A: IGDT-based optimization algorithm

